Supplementary material: Probing the effective Young's modulus of 'magic angle' inspired multi-functional twisted nano-heterostructures

T. Mukhopadhyay[a], A. Mahata[b], S. Naskar[c], S. Adhikari[d]

[a]*Department of Aerospace Engineering, Indian Institute of Technology Kanpur, Kanpur, India*
[b]*School of Engineering, Brown University, Providence, Rhode Island, USA*
[c]*Department of Aerospace Engineering, Indian Institute of Technology Bombay, Bombay, India*
[d]*College of Engineering, Swansea University, Swansea, UK*

Contents

1. Introduction

Generalized closed-form analytical formulae for the Young's moduli of twisted nano-heterostructures are developed based on the concept of a linkage between the molecular mechanics parameters and structural mechanics parameters of the interatomic bonds. The molecular mechanics based approach for obtaining equivalent elastic properties of atomic bonds is well-documented in scientific literature [1–4]. Therefore, the main contribution of this article lies in proposing computationally efficient and generalized analytical formulae for the elastic properties of twisted nano-heterostructures.

We follow a multi-stage bottom-up approach to develop the closed-form formulae for Young's moduli. The multi-layer twisted heterostructure can be idealized as a layered plate-like structural element with respective effective elastic properties and geometric dimensions (such as thickness) of each layer. Each of the layers are considered to be bonded perfectly with adjacent layers (refer to figure 3 of the main manuscript). Note that we consider two axis systems in the subsequent derivations: a local x-y-z system for each layer and a global 1-2-3 system for the entire heterostructure. The angle between x-y axis and 1-2 axis for a particular layer represent the twist, as shown in figure 3C of the main manuscript. The axis along directions z and 3 coincide with each other along thickness of the heterostructure. The effective elastic moduli (along the local axis system x-y) of each individual layer are determined first based on a mechanics based approach using the mechanical equivalence of bond properties. The Young's moduli of each layer in the global axis system 1-2 are obtained thereafter. Finally, the equivalent Young's moduli of the entire heterostructure is determined based on force equilibrium and deformation compatibility conditions at the last stage.

In this supplementary document, we systematically present the analytical formulation according to chronological stages of theoretical development: I. establishing the mechanical equivalence between molecular mechanics and structural mechanics parameters of atomic bonds for idealization of atomic bonds as circular beams, II. developing mathematical expressions for equivalent elastic moduli of untwisted single-layer 2D material lattices based on the mechanical properties of atomic bonds (i.e. idealized beams), III. development of the formulation for equivalent Young's moduli of twisted single-layer 2D materials using the elastic properties of single-layer untwisted 2D materials, IV. proposing generic closed-form formulae for equivalent Young's moduli of twisted multi-layer heterostructures using the Young's moduli of single-layer twisted 2D materials.

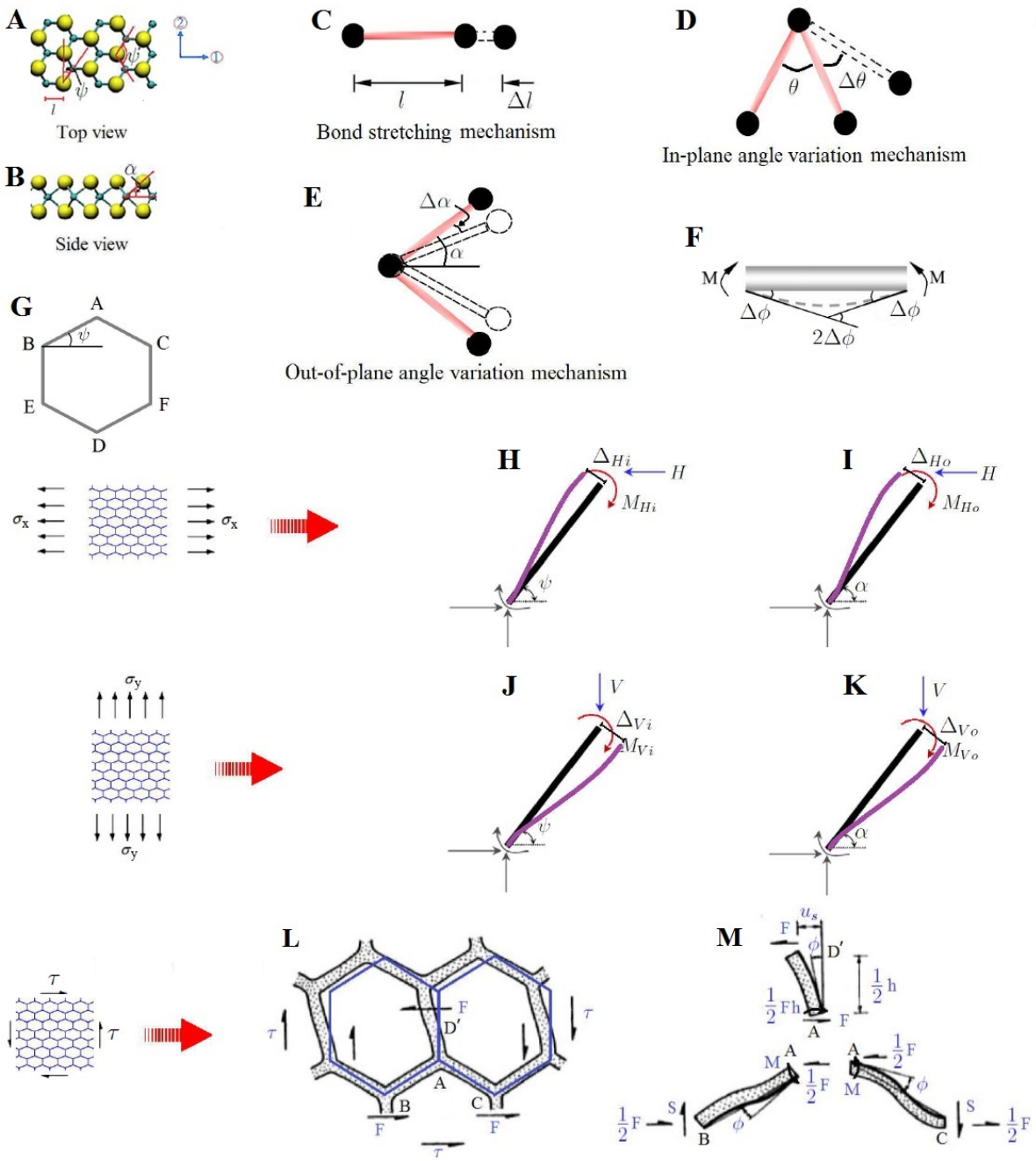

Figure S1: Deformation mechanics of inter-atomic bonds. **(A–B)** Top view and side view of a generic multiplanar hexagonal nanostructure. The in-plane angles (ψ and ψ') and out-of-plane angle (α) are indicated, wherein $\psi = 90° - \psi'\backslash 2$. It may be noted that different combinations of mono-planar and multi-planar structures with homogeneous and heterogeneous atomic distributions could be obtained as special cases of this generic nano-structure by considering the appropriate value of out-of-plane angle and necessary arrangement of atoms. **(C)**Bond stretching mechanism **(D)** In-plane angle variation mechanism **(E)** Out-of-plane angle variation mechanism **(F)** Bending deformation of an idealized beam element. Note that the in-plane and out-of-plane angle variations ($\Delta\theta$ and $\Delta\alpha$) are equivalent to the effective bending angle $2\Delta\phi$. **(G)** Top view of an idealized generic unit cell **(H)** Free body diagram of member AB for in-plane deformation under the application of force in direction x **(I)** Free body diagram of member AB for out-of-plane deformation under the application of force in direction x **(J)** Free body diagram of member AB for in-plane deformation under the application of force in direction y **(K)** Free body diagram of member AB for out-of-plane deformation under the application of force in direction y **(L–M)** Top view of a multi-planar hexagonal lattice for deriving the in-plane shear modulus.

2. Mechanical equivalence of atomic bonds: Bridging the relationship between molecular mechanics and structural mechanics parametrs

In this section, we present the mechanical equivalence of atomic bonds and equivalent beams that form the 2D material lattice-like structure. For atomic level behaviour of nano-scale materials, the total interatomic potential energy can be expressed as the sum of various individual energy terms related to bonding and non-bonding interactions [1]. Total strain energy (E) is expressed as the sum of energy contributions from bending of bonds (E_b), stretching of bonds (E_s), torsion of bonds (E_t) and energies associated with non-bonded terms (E_{nb}) such as the van der Waals attraction, the core repulsions and the coulombic energy (refer to figure 1(H–I) of the main manuscript).

$$E = E_s + E_b + E_t + E_{nb} \tag{1}$$

However, among all the energy components, effect of bending and stretching are predominant in case of small deformation [2, 4]. For the multiplanar hexagonal nano-structures (such as stanene and MoS_2), the strain energy caused by bending consists of two components, in-plane component (E_{bI}) and out-of-plane component (E_{bO}). The predominant deformation mechanisms for a multiplanar nanostructure are depicted in figure S1(C–E). It can be noted that the out-of-plane component becomes zero for monoplanar nanostructures such as graphane and hBN. The total inter-atomic potential energy (E) can be expressed as

$$\begin{aligned} E &= E_s + E_{bI} + E_{bO} \\ &= \frac{1}{2}k_r(\Delta l)^2 + \left(\frac{1}{2}k_\theta(\Delta\theta)^2 + \frac{1}{2}k_\theta(\Delta\alpha)^2\right) \end{aligned} \tag{2}$$

where Δl, $\Delta\theta$ and $\Delta\alpha$ denote the change in bond length, in-plane angle and out-of-plane angle respectively, as shown in figure S1. The quantities k_r and k_θ are the force constants associated with bond stretching and bond bending respectively. The first term in Equation 2 corresponds to strain energy due to stretching (E_s), while the terms within bracket represent the strain energies due to in-plane (E_{bI}) and out-of-plane (E_{bO}) angle variations, respectively. The force constants of the atomic bonds (k_r and k_θ) can be expressed in the form of structural equivalence using an equivalent mechanical beam. It can be noted that the stretching behaviour of an atomic bond and the equivalent beam is similar as shown in figure S1(C)). The behaviour of bending of the atomic bonds and the equivalent beam are presented in figure S1(D–E)) and figure S1(F)), respectively. In case of the atomic bonds, the effect of bending can be quantified as the change in bond angle as shown in figure S1(D–E)) (i.e. $\Delta\theta$ and $\Delta\alpha$ for in-plane and out-of-plane bending, respectively). For bending of the equivalent beam, the total relative change

in the angular direction of the two ends is $2\Delta\phi$. Thus, for bending deformation $2\Delta\phi$ is equivalent to $\Delta\theta$ (in-plane) and $\Delta\alpha$ (out-of-plane).

As per the standard theory of classical structural mechanics, strain energy of a uniform circular beam with cross-sectional area A, length l, Young's modulus E, and second moment of area I, under the application of a pure axial force N can be expressed as

$$U_a = \frac{1}{2}\int_0^L \frac{N^2}{EA}\,\mathrm{d}l = \frac{1}{2}\frac{N^2 l}{EA} = \frac{1}{2}\frac{EA}{l}(\Delta l)^2 \tag{3}$$

The strain energies due to pure bending moment M (refer to figure S1(F)) can be written as

$$U_b = \frac{1}{2}\int_0^L \frac{M^2}{EI}\,\mathrm{d}l = \frac{1}{2}\frac{EI}{l}(2\Delta\phi)^2 \tag{4}$$

Comparing Equation 3 with the expression for strain energy due to stretching (E_s) (refer Equation 2), it can be concluded that $K_r = \dfrac{EA}{l}$. As for bending, it is reasonable to assume that $2\Delta\phi$ is equivalent to $\Delta\theta$ and $\Delta\alpha$ (for in-plane and out-of-plane angle variations respectively), the following relation can be obtained: $k_\theta = \dfrac{EI}{l}$ (comparing Equation 4 with the expressions for the strain energies due to in-plane (E_{bI}) and out-of-plane (E_{bO}) angle variations). On the basis of the established mechanical equivalence between molecular mechanics parameters (k_r and k_θ) and structural mechanics parameters (EA and EI), the effective elastic moduli of twisted nano-heterostructures are obtained in the following sections.

3. Elastic moduli of a single-layer untwisted 2D material

In this section we derive the equivalent elastic properties of a single-layer 2D material along the local axis system x-y. The nano-structure of the 2D materials can be idealized as a lattice network made of equivalent mechanical beam elements. A unit cell based approach is utilized here to obtain the equivalent elastic properties of the entire lattices.

3.1. Young's modulus E_x

One hexagonal unit cell is considered to derive the expression for Young's moduli of the entire hexagonal periodic nano-structure as shown in figure S1G. Because of structural symmetry, horizontal deformation of the unit cell can be obtained by analysing the member AB only. The total horizontal deformation of the member AB (horizontal deflection of one end of the member with respect to the other end) under the application of stress σ_x has three components: axial deformation (δ_{aH}), bending deformation due to in-plane loading (δ_{bHi}) and bending deformation due to out-of-plane loading (δ_{bHo}).

$$\begin{aligned}\delta_{Hxx} &= \delta_{aH} + \delta_{bHi} + \delta_{bHo} \\ &= \frac{Hl\cos^2\psi\cos^2\alpha}{AE} + \frac{Hl^3\sin^2\psi}{12EI} + \frac{Hl^3\cos^2\psi\sin^2\alpha}{12EI}\end{aligned} \tag{5}$$

where $A = \frac{\pi d^2}{4}$, $I = \frac{\pi d^4}{64}$ and $H = \sigma_x tl(1+\sin\psi)\cos\alpha$. The parameters l and d represent length and diameter of the member AB respectively, while t is the thickness of single layer of such periodic structural form. The three parts of Equation 5 are derived by considering the respective deformation components in direction-1. Figure S1(H – I) show the member AB using top-view and side-view respectively, wherein the horizontal load H acts at the node A in the x–y plane. Inclination angle of the member AB in the x–y plane and x–z plane are ψ and α respectively, as shown in figure S1(A – B). From figure S1H, it can be understood that the horizontal force H has two components: $Hsin\psi$ (acting in a direction perpendicular to the member AB in the x–y plane) and $Hcos\psi$ (acting in a direction perpendicular to the force $Hsin\psi$ in the x–y plane). The $Hsin\psi$ component will cause a bending deflection Δ_{Hi}. The component of Δ_{Hi} in direction-x is denoted as δ_{bHi} in Equation 5. Using the standard formula of structural mechanics (bending deflection of one end of a beam with respect to the other end: $\delta = \frac{PL^3}{12EI}$, where L is the length of the beam, P is the applied point load across the beam length) the component δ_{bHi} can be expressed as

$$\delta_{bHi} = \Delta_{Hi}sin\psi = \frac{Hsin\psi l^3}{12EI}sin\psi = \frac{Hl^3sin^2\psi}{12EI} \tag{6}$$

The $Hcos\psi$ force can be resolved in two different components in the plane perpendicular to the x–y plane. The component $Hcos\psi cos\alpha$ causes axial deformation of the member AB, while the other component $Hcos\psi sin\alpha$ results in the bending deformation Δ_{Ho} (as indicated in figure S1I). The horizontal component of Δ_{Ho} in the x–y plane is denoted as δ_{bHo} in the Equation 5. Thus we get

$$\delta_{bHo} = \Delta_{Ho}sin\alpha cos\psi = \frac{Hcos\psi sin\alpha l^3}{12EI}sin\alpha cos\psi = \frac{Hl^3cos^2\psi sin^2\alpha}{12EI} \tag{7}$$

The horizontal axial deformation component in the x–y plane caused by the force $Hcos\psi cos\alpha$ is denoted as δ_{aH} in the Equation 5. Thus we get

$$\delta_{aH} = \frac{Hcos\psi cos\alpha l}{AE}cos\psi cos\alpha = \frac{Hlcos^2\psi cos^2\alpha}{AE} \tag{8}$$

Using the relationship between molecular mechanics parameters (k_r and k_θ) and structural mechanics parameters (EA and EI), form Equation 5, the expression for strain in direction-x (due to loading in

direction-x) can be written as

$$\begin{aligned}\epsilon_{xx} &= \frac{\delta_{Hxx}}{l\cos\psi\cos\alpha} \\ &= \frac{\sigma_x tl(1+\sin\psi)}{l\cos\psi}\left(\frac{l^2}{12k_\theta}\left(\sin^2\psi+\cos^2\psi\sin^2\alpha\right)+\frac{\cos^2\psi\cos^2\alpha}{k_r}\right)\end{aligned} \tag{9}$$

On the basis of the basic definition of Young's modulus ($E_x = \frac{\sigma_x}{\epsilon_{xx}}$), the closed-form expression for Young's modulus in direction-x can be obtained as

$$E_x = \frac{\cos\psi}{t(1+\sin\psi)\left(\frac{l^2}{12k_\theta}\left(\sin^2\psi+\cos^2\psi\sin^2\alpha\right)+\frac{\cos^2\psi\cos^2\alpha}{k_r}\right)} \tag{10}$$

3.2. Young's modulus E_y

Total vertical deformation of the unit cell under the application of σ_y is consisted of the deformation of member AB (δ_{V1}) and member BE (δ_{V2}) in direction-y (refer to figure S1). Deflection of joint A in direction-2 with respect to joint B has three components: axial deformation (δ_{aV1}), bending deformation due to in-plane loading (δ_{bV1i}) and bending deformation due to out-of-plane loading (δ_{bV1o}).

$$\begin{aligned}\delta_{V1} &= \delta_{aV1}+\delta_{bV1i}+\delta_{bV1o} \\ &= \frac{Vl\sin^2\psi\cos^2\alpha}{AE}+\frac{Vl^3\cos^2\psi}{12EI}+\frac{Vl^3\sin^2\psi\sin^2\alpha}{12EI}\end{aligned} \tag{11}$$

where $V = \sigma_y tl\cos\psi\cos\alpha$. As the member BE is parallel to the y–z plane, deflection of joint B with respect to the joint E has two components: axial deformation (δ_{aV2}) and bending deformation due to out-of-plane loading (δ_{bV2o}). It can be noted that the force acting on the member BE is $2V$ as there are similar unit cells adjacent to the one being analysed.

$$\begin{aligned}\delta_{V2} &= \delta_{aV2}+\delta_{bV2o} \\ &= \frac{2Vl\cos^2\alpha}{AE}+\frac{2Vl^3\sin^2\alpha}{12EI}\end{aligned} \tag{12}$$

Replacing the expressions of V, A, I, AE and EI, the total deformation in direction-y can be obtained from Equation 11 and 12 as

$$\begin{aligned}\delta_{Vyy} &= \delta_{V1}+\delta_{V2} \\ &= \sigma_y tl\cos\psi\cos\alpha\left(\frac{l^2}{12k_\theta}\left(\cos^2\psi+\sin^2\psi\sin^2\alpha+2\sin^2\alpha\right)+\frac{\cos^2\alpha}{k_r}\left(\sin^2\psi+2\right)\right)\end{aligned} \tag{13}$$

From Equation 13, the strain in direction-y (due to loading in direction-y) can be expresses as

$$\begin{aligned}\epsilon_{yy} &= \frac{\delta_{Vyy}}{(l+l\sin\psi)\cos\alpha} \\ &= \frac{\sigma_y t\cos\psi}{1+\sin\psi}\left(\frac{l^2}{12k_\theta}\left(\cos^2\psi+\sin^2\psi\sin^2\alpha+2\sin^2\alpha\right)+\frac{\cos^2\alpha}{k_r}\left(\sin^2\psi+2\right)\right)\end{aligned} \tag{14}$$

On the basis of the basic definition of Young's modulus ($E_y = \frac{\sigma_y}{\epsilon_{yy}}$), the closed-form expression for Young's modulus in direction-y can be obtained as

$$E_y = \frac{1+\sin\psi}{t\cos\psi\left(\frac{l^2}{12k_\theta}\left(\cos^2\psi+\sin^2\psi\sin^2\alpha+2\sin^2\alpha\right)+\frac{\cos^2\alpha}{k_r}\left(\sin^2\psi+2\right)\right)} \tag{15}$$

The Young's moduli (E_x and E_y) of a 2D material with hexagonal nano-structure can be predicted using the closed-form formulae (Equation 10 and 15) from molecular mechanics parameters (k_r and k_θ), bond length (l), bond angle (θ) and out-of-plane angle (α), which are available in the molecular mechanics literature.

3.3. Poisson's ratio ν_{xy}

In-plane Poisson's ratio for the loading direction-x (ν_{xy}) can be obtained as

$$\nu_{xy} = -\frac{\epsilon_{xy}}{\epsilon_{xx}} \tag{16}$$

where ϵ_{xy} and ϵ_{xx} are the strains in direction-y and direction-x respectively due to loading in direction-x. The expression for ϵ_{xx} is given in Equation 9. Derivation for the expression of ϵ_{xy} is provided next. The deformation in direction-y due to loading in direction-x can be obtained by considering one hexagonal unit cell as shown in figure S1. Because of structural symmetry, deformation in direction-y of the unit cell due to loading in direction-x can be obtained by analysing the member AB only. The total deformation in direction-y of the member AB (deflection in direction-y of one end of the member with respect to the other end) under the application of stress σ_x has two components: bending deformation due to in-plane loading (δ_{bVix}) and bending deformation due to out-of-plane loading (δ_{bVox}).

$$\begin{aligned}\delta_{Hxy} &= \delta_{bVix} + \delta_{bVox} \\ &= -\frac{Hl^3\sin\psi\cos\psi}{12EI} + \frac{Hl^3\sin\psi\cos\psi\sin^2\alpha}{12EI} \\ &= -\frac{Hl^3\sin\psi\cos\psi\cos^2\alpha}{12EI}\end{aligned} \tag{17}$$

Using the relationship between molecular mechanics parameter k_θ and structural mechanics parameter EI, form Equation 17, the expression for strain in direction-y (due to loading in direction-x) can be written as

$$\begin{aligned}\epsilon_{xy} &= \frac{\delta_{Hxy}}{(l+l\sin\psi)\cos\alpha} \\ &= -\frac{Hl\sin\psi\cos\psi\cos\alpha}{12k_\theta\left(1+\sin\psi\right)}\end{aligned} \tag{18}$$

On the basis of the basic definition of ν_{xy} as shown in Equation 16, the closed-form expression of in-plane Poisson's ratio for the loading direction-x can be obtained as

$$\nu_{xy} = \frac{\sin\psi\cos^2\psi\cos^2\alpha l^2}{12k_\theta\left(1+\sin\psi\right)\left(\frac{l^2}{12k_\theta}\left(\sin^2\psi+\cos^2\psi\sin^2\alpha\right)+\frac{\cos^2\psi\cos^2\alpha}{k_r}\right)} \tag{19}$$

3.4. Poisson's ratio ν_{yx}

In-plane Poisson's ratio for the loading direction-y (ν_{yx}) can be obtained as

$$\nu_{yx} = -\frac{\epsilon_{yx}}{\epsilon_{yy}} \tag{20}$$

where ϵ_{yx} and ϵ_{yy} are the strains in direction-x and direction-y respectively due to loading in direction-y. The expression for ϵ_{yy} is given in Equation 14. Derivation for the expression of ϵ_{yx} is provided next. The deformation in direction-x due to loading in direction-y can be obtained by considering one hexagonal unit cell as shown in figure S1. Because of structural symmetry, deformation in direction-x of the unit cell due to loading in direction-y can be obtained by analysing the member AB only. The total deformation in direction-x of the member AB (deflection in direction-x of one end of the member with respect to the other end) under the application of stress σ_y has two components: bending deformation due to in-plane loading (δ_{bHiy}) and bending deformation due to out-of-plane loading (δ_{bHoy}).

$$\begin{aligned}\delta_{Hyx} &= \delta_{bHiy} + \delta_{bHoy} \\ &= -\frac{Vl^3\sin\psi\cos\psi}{12EI} + \frac{Vl^3\sin\psi\cos\psi\sin^2\alpha}{12EI} \\ &= -\frac{Vl^3\sin\psi\cos\psi\cos^2\alpha}{12EI}\end{aligned} \tag{21}$$

Using the relationship between molecular mechanics parameter k_θ and structural mechanics parameter EI, form Equation 21, the expression for strain in direction-x (due to loading in direction-y) can be written as

$$\begin{aligned}\epsilon_{yx} &= \frac{\delta_{Hyx}}{l\cos\psi\cos\alpha} \\ &= -\frac{Vl\sin\psi\cos\alpha}{12k_\theta}\end{aligned} \tag{22}$$

On the basis of the basic definition of ν_{yx} as shown in Equation 20, the closed-form expression of in-plane Poisson's ratio for the loading direction-y can be obtained as

$$\nu_{yx} = \frac{\sin\psi\left(1+\sin\psi\right)\cos^2\alpha l^2}{12k_\theta\left(\frac{l^2}{12k_\theta}\left(\cos^2\psi+\sin^2\psi\sin^2\alpha+2\sin^2\alpha\right)+\frac{\cos^2\alpha}{k_r}\left(\sin^2\psi+2\right)\right)} \tag{23}$$

3.5. Shear modulus G_{xy}

For deriving the in-plane shear modulus of multi-planar hexagonal nanostructures, the free body diagram shown in figure S1(L–M) is analysed. It can be noted here that the top view is shown in this figure and the individual constituent members are inclined at an angle α with the x–y plane. From the free body diagram

$$M = \frac{Fl\cos\alpha}{4} \tag{24}$$

where $F = 2\tau l^2 \cos\psi \cos\alpha \sin\alpha$. Deflection of the end A with respect to the end C due to application of moment M at the end A is given as

$$\delta_0 = \frac{Ml^2}{6EI} \tag{25}$$

Thus the rotation of joint A can be expressed as

$$\begin{aligned} \phi &= \frac{\delta_0}{l} \\ &= \frac{Fl^2\cos\alpha}{24EI} \end{aligned} \tag{26}$$

Deformation of point D′ in direction - x due to rotation of the joint A is

$$\delta_r = \frac{1}{2}\phi l = \frac{Fl^3\cos\alpha}{48EI} \tag{27}$$

The bending deformation of the member AD′ in direction - x can be expressed as

$$\delta_b = \frac{Fl^3}{24EI} \tag{28}$$

The total shear deformation due to bending of the member AD′ and rotation of the joint A is given by

$$u_s = \delta_b + \delta_r = \frac{Fl^3}{48EI}\left(\cos\alpha + 2\right) \tag{29}$$

The axial deformation of members AB and AC caused by the force S will also contribute to the total shear deformation, where $S = \tau l^2 \sin\alpha\cos\alpha(1+\sin\psi)$. Comparing the expression of τ, obtained from the expressions of F and S

$$S = \frac{F(1+\sin\psi)}{2\cos\psi} \tag{30}$$

Axial deformation of the member AB can be expressed as

$$\begin{aligned} \delta_a &= \frac{\left(S\sin\psi + \frac{F}{2}\cos\psi\right)\cos\alpha l\cos\alpha\sin\psi}{AE} \\ &= \frac{Fl\sin\psi(1+\sin\psi)\cos^2\alpha}{2AE\cos\psi} \end{aligned} \tag{31}$$

Thus the shear strain caused by bending (γ_b) and axial (γ_a) deformations can be expressed as

$$\begin{aligned}\gamma &= \gamma_a + \gamma_b \\ &= 2\left(\frac{2\delta_a}{2l\cos\psi\cos\alpha} + \frac{u_s}{l(1+\sin\psi)\cos\alpha}\right) \\ &= \tau l^2 \cos\psi\cos\alpha\sin\alpha\left(\frac{\sin\psi(1+\sin\psi)}{AE\cos^2\psi} + \frac{l^2(\cos\alpha+2)}{6EI(1+\sin\psi)\cos\alpha}\right)\end{aligned} \tag{32}$$

Replacing the structural mechanics parameters EI and AE by the molecular mechanics parameters k_θ and k_r respectively in the above equation, the expression for in-plane shear modulus can be expressed as

$$\begin{aligned}G_{xy} &= \frac{\tau}{\gamma} \\ &= \frac{k_r k_\theta \cos\psi(1+\sin\psi)}{t\left(k_\theta \sin\psi(1+\sin\psi)^2\cos\alpha + \dfrac{k_r l^2}{6}\cos^2\psi(\cos\alpha+2)\right)}\end{aligned} \tag{33}$$

4. Young's moduli of twisted single-layer 2D materials

In the preceding section, the equivalent elastic properties of a single-layer 2D material are obtained in the local axis system x–y. In this section, we derive the expressions of the two Young's moduli in the global axis system of the entire heterostructure i.e. the 1–2 axis (refer to figure 3C of the main paper).

Let us consider the in-plane elastic properties of a thin two-dimensional equivalent plate-like structure, which can be thought as an idealization of the actual 2D material lattice. The elements of the stress and strain vectors of the equivalent plate-like structure are related through the compliance matrix $\mathbf{S}$ as (in the local axis system x–y)

$$\boldsymbol{\varepsilon}_m = \mathbf{S}\boldsymbol{\sigma}_m \tag{34}$$

Here the strain vector, the compliance matrix and the stress vector are given by (in the local axis system x–y)

$$\boldsymbol{\varepsilon}_m = \begin{Bmatrix}\varepsilon_x \\ \varepsilon_y \\ \gamma_{xy}\end{Bmatrix}, \quad \mathbf{S} = \begin{bmatrix}S_{xx} & S_{xy} & 0 \\ S_{xy} & S_{yy} & 0 \\ 0 & 0 & S_{66}\end{bmatrix} \quad \text{and} \quad \boldsymbol{\sigma}_m = \begin{Bmatrix}\sigma_x \\ \sigma_y \\ \tau_{xy}\end{Bmatrix} \tag{35}$$

The compliance matrix is a 3×3 vector-matrix system. The (3,3) element of the compliance matrix is denoted by (66). This notation is adopted from a more general treatment of the constitutive equation from an orthotropic material point of view. The elements of the compliance matrix can be related to the effective elastic properties (as presented in the preceding section) of the 2D material (or, equivalent

plate-like structure) in the local x–y axis system as

$$S_{xx} = \frac{1}{E_x}, \qquad S_{yy} = \frac{1}{E_y} \tag{36}$$

$$S_{xy} = -\frac{\nu_{xy}}{E_x} = -\frac{\nu_{yx}}{E_y}, \quad S_{66} = \frac{1}{G_{xy}} \tag{37}$$

Here E_x and E_y are the Young's moduli in the 'x' and 'y' directions as shown in figure 3C of the main paper, G_{xy} is the shear modulus and ν_{xy}, ν_{yx} are the two Poisson's ratios.

We use the subscript $(\bullet)_m$ to denote properties of the original materials in local x–y coordinate system and subscript $(\bullet)_p$ to denote properties of the heterostructure in a global co-ordinate system 1–2. Our objective here is to convert the effective Young's moduli obtained in the local x–y system to the global 1–2 system, where the twisting angle between these two axis systems is θ (refer to figure 3C of the main paper). Using the second-order transformation matrix for the rotation of angle θ, the stress and strain vectors in the two coordinate systems are related as

$$\boldsymbol{\sigma}_m = \mathbf{T}(\theta)\boldsymbol{\sigma}_p \quad \text{and} \quad \boldsymbol{\varepsilon}_m = \mathbf{T}(\theta)\boldsymbol{\varepsilon}_p \tag{38}$$

Here the second-order transformation matrix is given by

$$\mathbf{T}(\theta) = \begin{bmatrix} (\cos(\theta))^2 & (\sin(\theta))^2 & 2\sin(\theta)\cos(\theta) \\ (\sin(\theta))^2 & (\cos(\theta))^2 & -2\sin(\theta)\cos(\theta) \\ -\sin(\theta)\cos(\theta) & \sin(\theta)\cos(\theta) & (\cos(\theta))^2 - (\sin(\theta))^2 \end{bmatrix} \tag{39}$$

Using equations (34) and (38), we can deduce the stress-strain relationship in the $1-2$ coordinate system as

$$\boldsymbol{\sigma}_p = \mathbf{T}^{-1}(\theta)\boldsymbol{\sigma}_m \quad \text{or} \quad \boldsymbol{\sigma}_p = \mathbf{T}^{-1}(\theta)\mathbf{S}^{-1}\boldsymbol{\varepsilon}_m \quad \text{or} \quad \boldsymbol{\sigma}_p = \mathbf{T}^{-1}(\theta)\mathbf{S}^{-1}\mathbf{T}(\theta)\boldsymbol{\varepsilon}_p \tag{40}$$

Inverting this matrix equation we have

$$\boldsymbol{\varepsilon}_p = \underbrace{\mathbf{T}^{-1}(\theta)\mathbf{S}\mathbf{T}(\theta)}_{\overline{\mathbf{S}}}\boldsymbol{\sigma}_p \tag{41}$$

Comparing this equation with the stress-strain equation (34), we can consider that the transformed compliance matrix is given by

$$\overline{\mathbf{S}} = \mathbf{T}^{-1}(\theta)\mathbf{S}\mathbf{T}(\theta) \tag{42}$$

Comparing the elements of this transformed compliance matrix with equation (36) we can deduce that

$$\overline{S}_{11} = \frac{1}{E_{1s}}, \qquad \overline{S}_{22} = \frac{1}{E_{2s}} \tag{43}$$

The subscripts 's' in the above equations are added to denote the properties corresponding to a single layer. Performing the matrix multiplications in Equation 42, we obtain the Young's moduli of a single twisted layer in the global coordinate system as

$$\frac{1}{E_{1s}} = \overline{S}_{11} = \left(\frac{(\cos(\theta))^2}{E_x} - \frac{(\sin(\theta))^2 \nu_{yx}}{E_y} \right) (\cos(\theta))^2 + \left(-\frac{(\cos(\theta))^2 \nu_{xy}}{E_x} + \frac{(\sin(\theta))^2}{E_y} \right) (\sin(\theta))^2 + 2 \frac{(\sin(\theta))^2 (\cos(\theta))^2}{G_{xy}} \quad (44)$$

and

$$\frac{1}{E_{2s}} = \overline{S}_{22} = \left(\frac{(\sin(\theta))^2}{E_x} - \frac{(\cos(\theta))^2 \nu_{yx}}{E_y} \right) (\sin(\theta))^2 + \left(-\frac{(\sin(\theta))^2 \nu_{xy}}{E_x} + \frac{(\cos(\theta))^2}{E_y} \right) (\cos(\theta))^2 + 2 \frac{(\sin(\theta))^2 (\cos(\theta))^2}{G_{xy}} \quad (45)$$

From Equation 44 and 45 and noting that $E_x \nu_{yx} = E_y \nu_{xy}$ (refer to Equation 10, 15, 19 and 23), we get the final expressions of a single-layer twisted 2D material in the global axis system 1–2,

$$E_{1s} = \frac{1}{\left(\frac{\cos^4\theta}{E_x} + \frac{\sin^4\theta}{E_y} - 2\left(\frac{\nu_{xy}}{E_x} - \frac{1}{G_{xy}} \right) \sin^2\theta \cos^2\theta \right)} \quad (46)$$

$$E_{2s} = \frac{1}{\left(\frac{\sin^4\theta}{E_x} + \frac{\cos^4\theta}{E_y} - 2\left(\frac{\nu_{xy}}{E_x} - \frac{1}{G_{xy}} \right) \sin^2\theta \cos^2\theta \right)} \quad (47)$$

It may be noted in the above two equations that the Young's moduli of a 2D material lattice layer can be expressed in the global co-ordinate system 1–2 as a function of the elastic properties of the 2D material in the local co-ordinate system x–y (as derived in the preceding section). Since the global co-ordinate system 1–2 is common for all the layers in the heterostructure, we can combine the properties of each of the constituent layers to obtain the effective Young's moduli of the entire heterostructure ensuring equilibrium and compatibility conditions, as presented in the following section.

5. Young's moduli of twisted multi-layer nano-heterostructures

Equivalent elastic properties of the multi-layer twisted nano-heterostructures are derived based on a multi-stage idealization scheme as depicted in figure 3(A–B) of the main paper. The equivalent layer-wise properties in the global axis system for each twisted layer are used for this purpose [5]. Each of the layers are considered to be bonded perfectly with adjacent layers. The equivalent Young's moduli of the entire twisted heterostructure is determined based on force equilibrium and deformation compatibility

conditions as described here.

5.1. Effective Young's modulus in direction - 1 (E_1) for twisted nano-heterostructures

Figure 3D of the main paper shows the side view of an idealized three-layer twisted heterostructure with the stress applied in direction - 1. From the condition of force equilibrium, the total force applied in direction - 1 should be equal to the summation of the force component shared by each of the constituting layers in the same direction. Thus considering a heterostructure with n number of layers

$$\sigma_1 tB = \sum_{i=1}^{n} \sigma_{1i} t_i B \tag{48}$$

where $t = \sum_{i=1}^{n} t_i$; t_i represents the thickness of i^{th} layer ($i = 1, 2, 3...n$). From the definition of Young's modulus, the above expression can be written as

$$E_1 \epsilon_1 t = \sum_{i=1}^{n} E_{1si} \epsilon_{1si} t_i \tag{49}$$

where E_1 and ϵ_1 are the effective Young's modulus in direction - 1 and the strain in direction - 1 respectively for the entire heterostructure. E_{1si} and ϵ_{1si} represent the effective Young's modulus in direction - 1 and the strain in direction - 1 of i^{th} layer respectively. As each of the layers are considered to be perfectly bonded with the adjacent layers, the deformation compatibility condition yields: $\epsilon_1 = \epsilon_{1si}, \in [1, n]$. Thus Equation 49 and 10 give the expression of Young's modulus in direction - 1 for the entire twisted heterostructure as

$$\begin{aligned} E_1 &= \frac{1}{t} \sum_{i=1}^{n} E_{1si} t_i \\ &= \frac{1}{t} \sum_{i=1}^{n} \frac{1}{\left(\dfrac{\cos^4 \theta_i}{\bar{E}_{xi}} + \dfrac{\sin^4 \theta_i}{\bar{E}_{yi}} - 2 \left(\dfrac{\nu_{xyi}}{\bar{E}_{xi}} - \dfrac{1}{\bar{G}_{xyi}} \right) \sin^2 \theta_i \cos^2 \theta_i \right)} \end{aligned} \tag{50}$$

where $(\bar{\bullet}) = (\bullet) \times t$ in the above equation represents rigidity of the 2D material mono-layer in longitudinal, transverse and shear directions (i.e. $\bar{E}_{xi} = E_{xi} \times t_i$, $\bar{E}_{yi} = E_{yi} \times t_i$ and $\bar{G}_{xyi} = G_{xyi} \times t_i$). The subscript i in the above expression of E_1 indicates the parameters corresponding to the i^{th} layer. The expressions of E_{xi}, E_{yi}, ν_{xyi} and G_{xyi} are given in Equation 10, 15, 19 and 33, respectively.

5.2. Effective Young's modulus in direction - 2 (E_2) for twisted nano-heterostructures

Figure 3E of the main paper shows the side view of an idealized three-layer twisted heterostructure with the stress applied in direction - 2. From the condition of force equilibrium, the total force applied in direction - 2 should be equal to the summation of the force component shared by each of the constituting

layers in the same direction. Thus considering a heterostructure with n number of layers

$$\sigma_2 tL = \sum_{i=1}^{n} \sigma_{2i} t_i L \tag{51}$$

where $t = \sum_{i=1}^{n} t_i$; t_i represents the thickness of i^{th} layer ($i = 1, 2, 3...n$). From the definition of Young's modulus, the above expression can be written as

$$E_2 \epsilon_2 t = \sum_{i=1}^{n} E_{2si} \epsilon_{2si} t_i \tag{52}$$

where E_2 and ϵ_2 are the effective Young's modulus in direction - 2 and the strain in direction - 2 respectively for the entire heterostructure. E_{2si} and ϵ_{2si} represent the effective Young's modulus in direction - 2 and the strain in direction - 2 of i^{th} layer respectively. As each of the layers are considered to be perfectly bonded with the adjacent layers, the deformation compatibility condition yields: $\epsilon_2 = \epsilon_{2si}, \in [1, n]$. Thus Equation 52 and 15 give the expression of Young's modulus in direction - 2 for the entire twisted heterostructure as

$$\begin{aligned} E_2 &= \frac{1}{t} \sum_{i=1}^{n} E_{2si} t_i \\ &= \frac{1}{t} \sum_{i=1}^{n} \frac{1}{\left(\dfrac{\sin^4 \theta_i}{\bar{E}_{xi}} + \dfrac{\cos^4 \theta_i}{\bar{E}_{yi}} - 2 \left(\dfrac{\nu_{xyi}}{\bar{E}_{xi}} - \dfrac{1}{\bar{G}_{xyi}} \right) \sin^2 \theta_i \cos^2 \theta_i \right)} \end{aligned} \tag{53}$$

where $(\bar{\bullet}) = (\bullet) \times t$ in the above equation represents rigidity of the 2D material mono-layer in longitudinal, transverse and shear directions (i.e. $\bar{E}_{xi} = E_{xi} \times t_i$, $\bar{E}_{yi} = E_{yi} \times t_i$ and $\bar{G}_{xyi} = G_{xyi} \times t_i$). The subscript i in the above expression of E_2 indicates the parameters corresponding to the i^{th} layer. The expressions of E_{xi}, E_{yi}, ν_{xyi} and G_{xyi} are given in Equation 10, 15, 19 and 33, respectively.

6. Additional numerical results on the Young's moduli of twisted multi-layered heterostructures

In this section, we present additional numerical results for twisted nanostructures. These results can be viewed as complementary plots to the results presented in the main paper. Here we start by investigating single-layer 2D materials corresponding to different twisting angles as shown in figure S2. Interestingly, the trend of variations of Young's moduli for different 2D materials with respect to twisting angle is similar to that of bi-layer nanostructures made of same 2D materials (refer to figures 4 and 5 of the main paper). Figure S3 presents numerical results for Young's moduli of two-layer heterostructures with same material at both layers (considering hBN and stanene), wherein both the layers are twisted simultaneously.

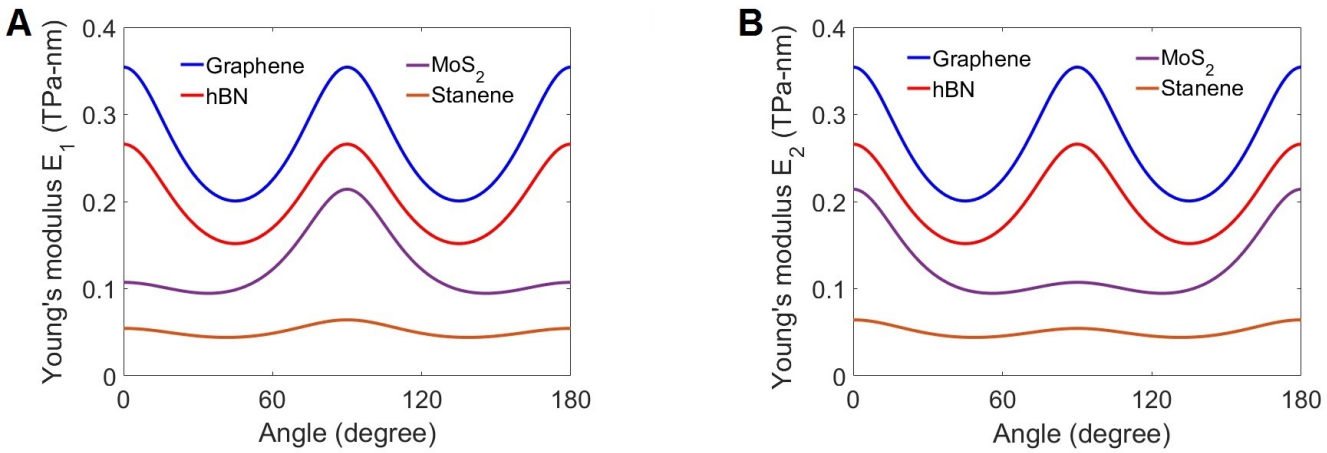

Figure S2: Young's modulus of a single layer rotated material. Young's moduli of rotated single-layer 2D materials at different angles (considering graphene, hBN, MoS_2 and stanene) **(A)** Young's modulus E_1 **(B)** Young's modulus E_2.

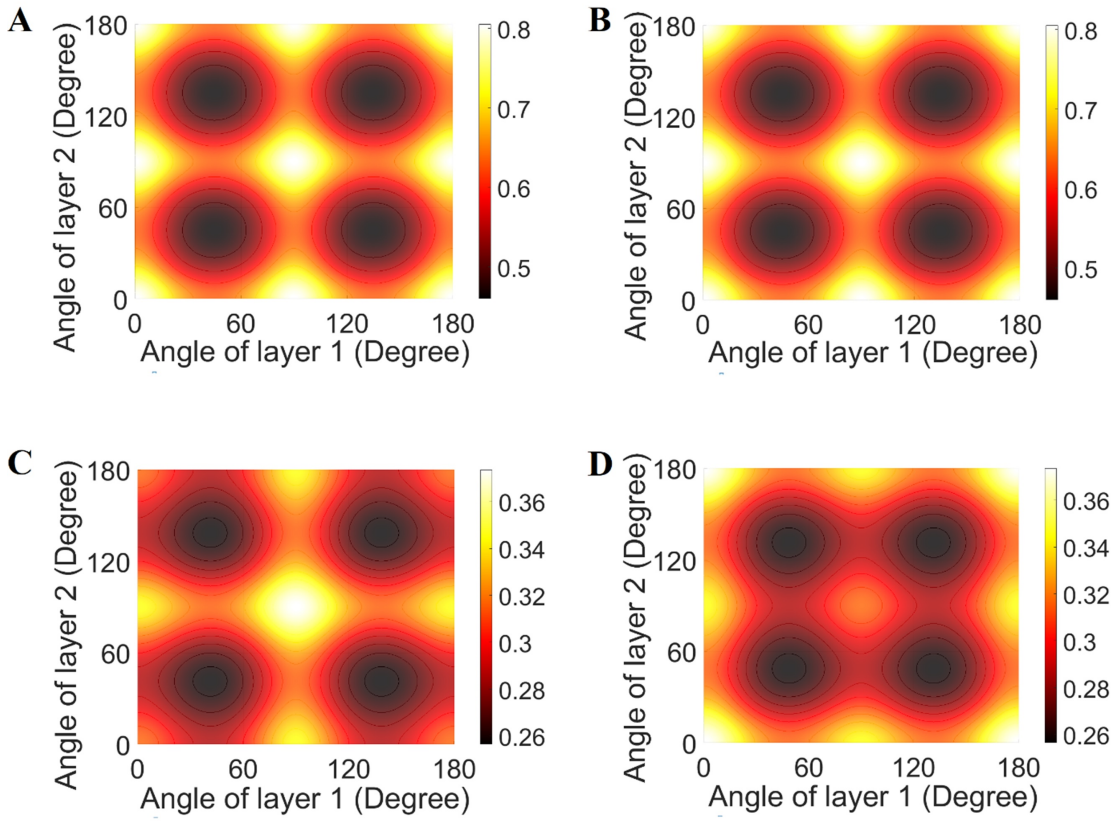

Figure S3: Young's modulus (TPa) of two-layer configurations with same material at both layers and both the layers rotated simultaneously. (A) Young's modulus E_1 of two-layer hBN nanostructure (H/H) with a configuration of $[\theta_1^\circ/\theta_2^\circ]$, where θ_1 and θ_2 represent the in-plane rotational angle of layer 1 and layer 2 respectively **(B)** Young's modulus E_2 of two-layer hBN nanostructure (H/H) with a configuration of $[\theta_1^\circ/\theta_2^\circ]$, where θ_1 and θ_2 represent the in-plane rotational angle of layer 1 and layer 2 respectively **(C)** Young's modulus E_1 of two-layer stanene nanostructure (S/S) with a configuration of $[\theta_1^\circ/\theta_2^\circ]$, where θ_1 and θ_2 represent the in-plane rotational angle of layer 1 and layer 2 respectively **(D)** Young's modulus E_2 of two-layer stanene nanostructure (S/S) with a configuration of $[\theta_1^\circ/\theta_2^\circ]$, where θ_1 and θ_2 represent the in-plane rotational angle of layer 1 and layer 2 respectively.

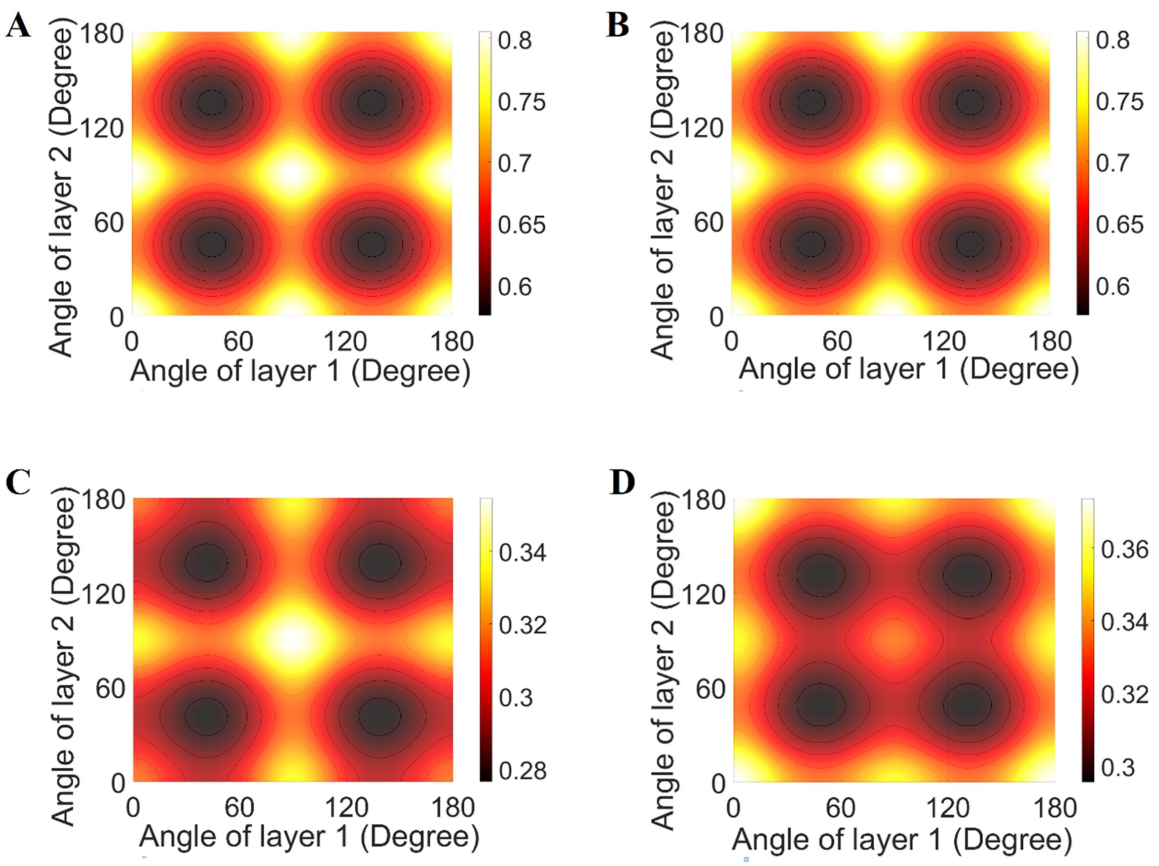

Figure S4: Young's modulus (TPa) of three-layer configurations with same material at all layers, where one of the layers has no rotation and the other two layers are rotated simultaneously. (A) Young's modulus E_1 of three-layer hBN nanostructure (H/H/H) with a configuration of $[0°/\theta_2°/\theta_3°]$, where θ_2 and θ_3 represent the in-plane rotational angle of layer 2 and layer 3 respectively **(B)** Young's modulus E_2 of three-layer hBN nanostructure (H/H/H) with a configuration of $[0°/\theta_2°/\theta_3°]$, where θ_2 and θ_3 represent the in-plane rotational angle of layer 2 and layer 3 respectively **(C)** Young's modulus E_1 of three-layer stanene nanostructure (S/S/S) with a configuration of $[0°/\theta_2°/\theta_3°]$, where θ_2 and θ_3 represent the in-plane rotational angle of layer 2 and layer 3 respectively **(D)** Young's modulus E_2 of three-layer stanene nanostructure (S/S/S) with a configuration of $[0°/\theta_2°/\theta_3°]$, where θ_2 and θ_3 represent the in-plane rotational angle of layer 2 and layer 3 respectively.

Figures S4 - S13 present numerical results for three-layer nanostructures in an increasing order of structural complexity. Figure S4 shows the variation of Young's moduli with respect to the twisting angles in two layers considering hBN and stanene, wherein all the three layers are composed of same material. The subsequent figures consider three-layer configurations where more than one type of 2D materials are used to form the heterostructure. Similar to the results presented in the main paper, it is observed that a definitive correlation between E_1 and E_2 exists depending on the nanostructural configuration. In case of multi-layered twisted nanostructures composed of same 2D material, corresponding to any particular twisting angle, we find $E_1 = E_2$ in case of monoplanar 2D materials, while $E_1 \neq E_2$ in case of multiplanar 2D materials. In general, the twisted or untwisted heterostructures with at least

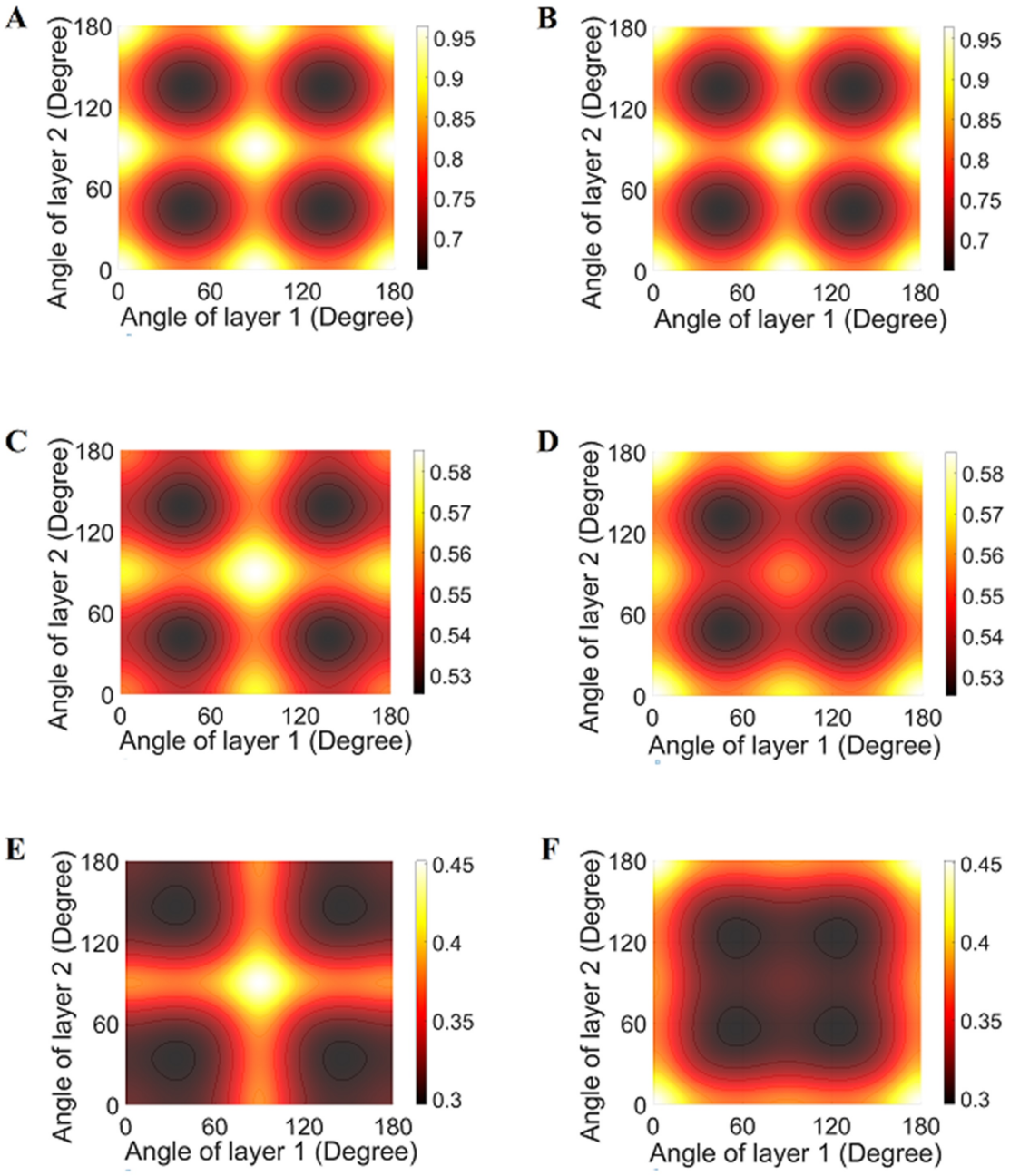

Figure S5: Young's modulus (TPa) of three-layer configurations, where hBN is at one of the layers without any rotation and the other two rotating layers are of same material other than hBN. (A) Young's modulus E_1 of three-layer hBN-graphene heterostructure (H/G/G) with a configuration of $[0°/\theta_2°/\theta_3°]$, where θ_2 and θ_3 represent the in-plane rotational angle of layer 2 and layer 3 respectively **(B)** Young's modulus E_2 of three-layer hBN-graphene heterostructure (H/G/G) with a configuration of $[0°/\theta_2°/\theta_3°]$, where θ_2 and θ_3 represent the in-plane rotational angle of layer 2 and layer 3 respectively **(C)** Young's modulus E_1 of three-layer hBN-stanene heterostructure (H/S/S) with a configuration of $[0°/\theta_2°/\theta_3°]$, where θ_2 and θ_3 represent the in-plane rotational angle of layer 2 and layer 3 respectively **(D)** Young's modulus E_2 of three-layer hBN-stanene heterostructure (H/S/S) with a configuration of $[0°/\theta_2°/\theta_3°]$, where θ_2 and θ_3 represent the in-plane rotational angle of layer 2 and layer 3 respectively **(E)** Young's modulus E_1 of three-layer hBN-MoS_2 heterostructure (H/M/M) with a configuration of $[0°/\theta_2°/\theta_3°]$, where θ_2 and θ_3 represent the in-plane rotational angle of layer 2 and layer 3 respectively **(F)** Young's modulus E_2 of three-layer hBN-MoS_2 heterostructure (H/M/M) with a configuration of $[0°/\theta_2°/\theta_3°]$, where θ_2 and θ_3 represent the in-plane rotational angle of layer 2 and layer 3 respectively.

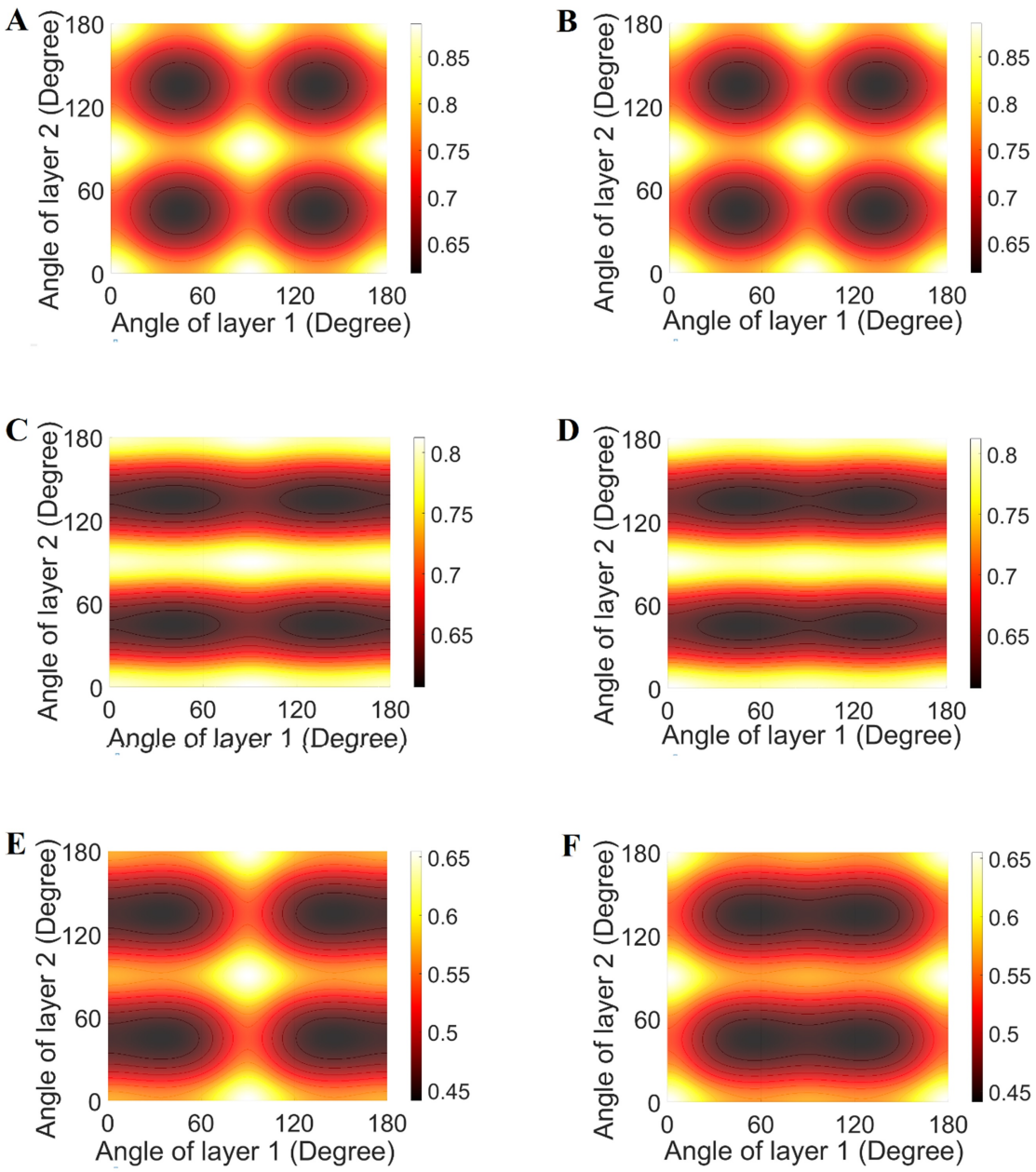

Figure S6: Young's modulus (TPa) of three-layer configurations, where hBN is at one of the layers without any rotation and one of the rotating layers is graphene. (A) Young's modulus E_1 of three-layer hBN-graphene heterostructure (H/G/H or H/H/G) with a configuration of $[0°/\theta_2°/\theta_3°]$, where θ_2 and θ_3 represent the in-plane rotational angle of layer 2 and layer 3 respectively **(B)** Young's modulus E_2 of three-layer hBN-graphene heterostructure (H/G/H or H/H/G) with a configuration of $[0°/\theta_2°/\theta_3°]$, where θ_2 and θ_3 represent the in-plane rotational angle of layer 2 and layer 3 respectively **(C)** Young's modulus E_1 of three-layer hBN-graphene-stanene heterostructure (H/G/S or H/S/G) with a configuration of $[0°/\theta_2°/\theta_3°]$, where θ_2 and θ_3 represent the in-plane rotational angle of layer 2 and layer 3 respectively **(D)** Young's modulus E_2 of three-layer hBN-graphene-stanene heterostructure (H/G/S or H/S/G) with a configuration of $[0°/\theta_2°/\theta_3°]$, where θ_2 and θ_3 represent the in-plane rotational angle of layer 2 and layer 3 respectively **(E)** Young's modulus E_1 of three-layer hBN-graphene-MoS_2 heterostructure (H/G/M or H/M/G) with a configuration of $[0°/\theta_2°/\theta_3°]$, where θ_2 and θ_3 represent the in-plane rotational angle of layer 2 and layer 3 respectively **(F)** Young's modulus E_2 of three-layer hBN-graphene-MoS_2 heterostructure (H/G/M or H/M/G) with a configuration of $[0°/\theta_2°/\theta_3°]$, where θ_2 and θ_3 represent the in-plane rotational angle of layer 2 and layer 3 respectively.

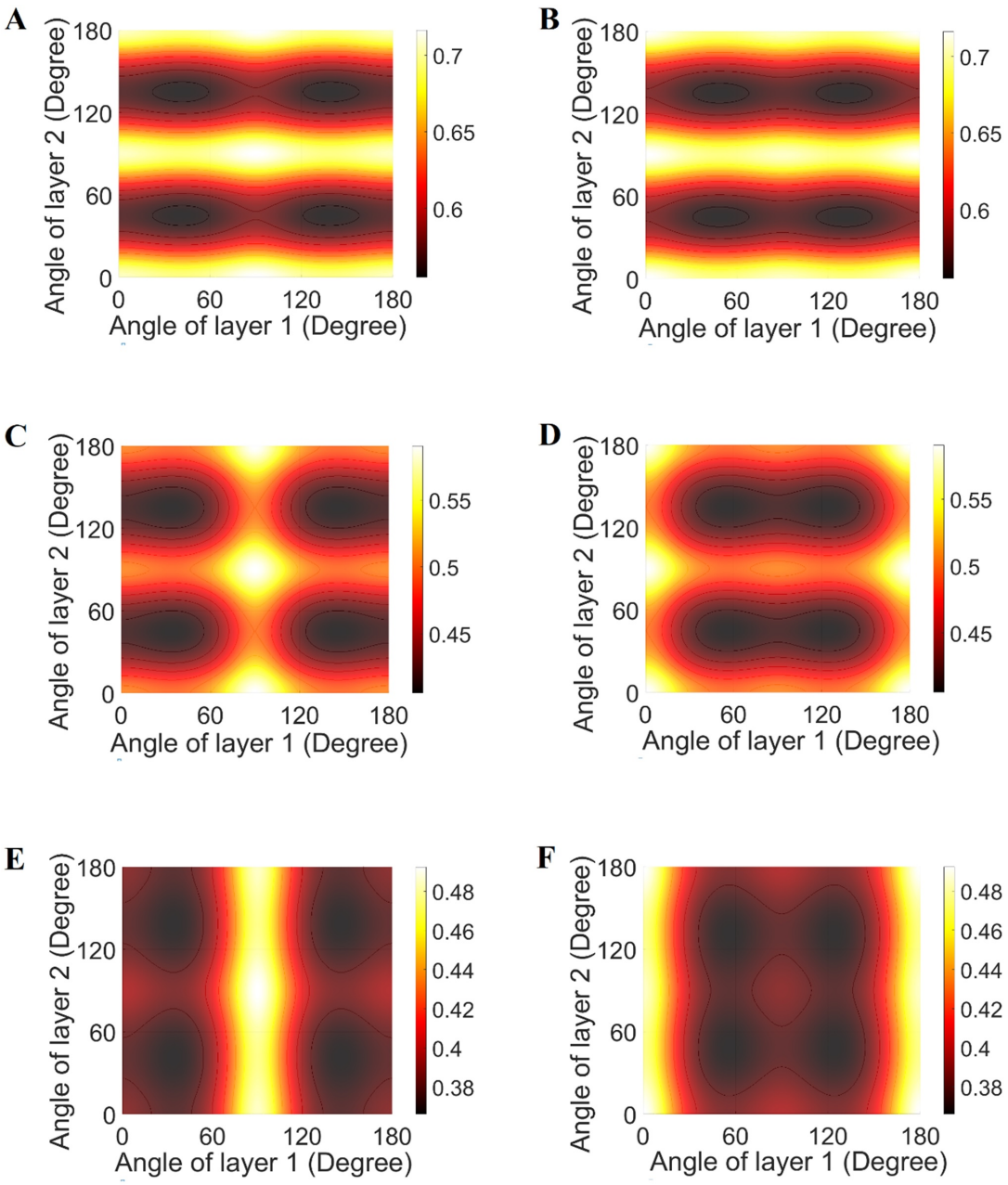

Figure S7: Young's modulus (TPa) of three-layer configurations, where hBN is at one of the layers without any rotation and the other two rotating layers are of two different materials other than graphene. (A) Young's modulus E_1 of three-layer hBN-stanene heterostructure (H/H/S or H/S/H) with a configuration of $[0°/\theta_2°/\theta_3°]$, where θ_2 and θ_3 represent the in-plane rotational angle of layer 2 and layer 3 respectively **(B)** Young's modulus E_2 of three-layer hBN-stanene heterostructure (H/H/S or H/S/H) with a configuration of $[0°/\theta_2°/\theta_3°]$, where θ_2 and θ_3 represent the in-plane rotational angle of layer 2 and layer 3 respectively **(C)** Young's modulus E_1 of three-layer hBN-MoS_2 heterostructure (H/H/M or H/M/H) with a configuration of $[0°/\theta_2°/\theta_3°]$, where θ_2 and θ_3 represent the in-plane rotational angle of layer 2 and layer 3 respectively **(D)** Young's modulus E_2 of three-layer hBN-MoS_2 heterostructure (H/H/M or H/M/H) with a configuration of $[0°/\theta_2°/\theta_3°]$, where θ_2 and θ_3 represent the in-plane rotational angle of layer 2 and layer 3 respectively **(E)** Young's modulus E_1 of three-layer hBN-stanene-MoS_2 heterostructure (H/S/M or H/M/S) with a configuration of $[0°/\theta_2°/\theta_3°]$, where θ_2 and θ_3 represent the in-plane rotational angle of layer 2 and layer 3 respectively **(F)** Young's modulus E_2 of three-layer hBN-stanene-MoS_2 heterostructure (H/S/M or H/M/S) with a configuration of $[0°/\theta_2°/\theta_3°]$, where θ_2 and θ_3 represent the in-plane rotational angle of layer 2 and layer 3 respectively.

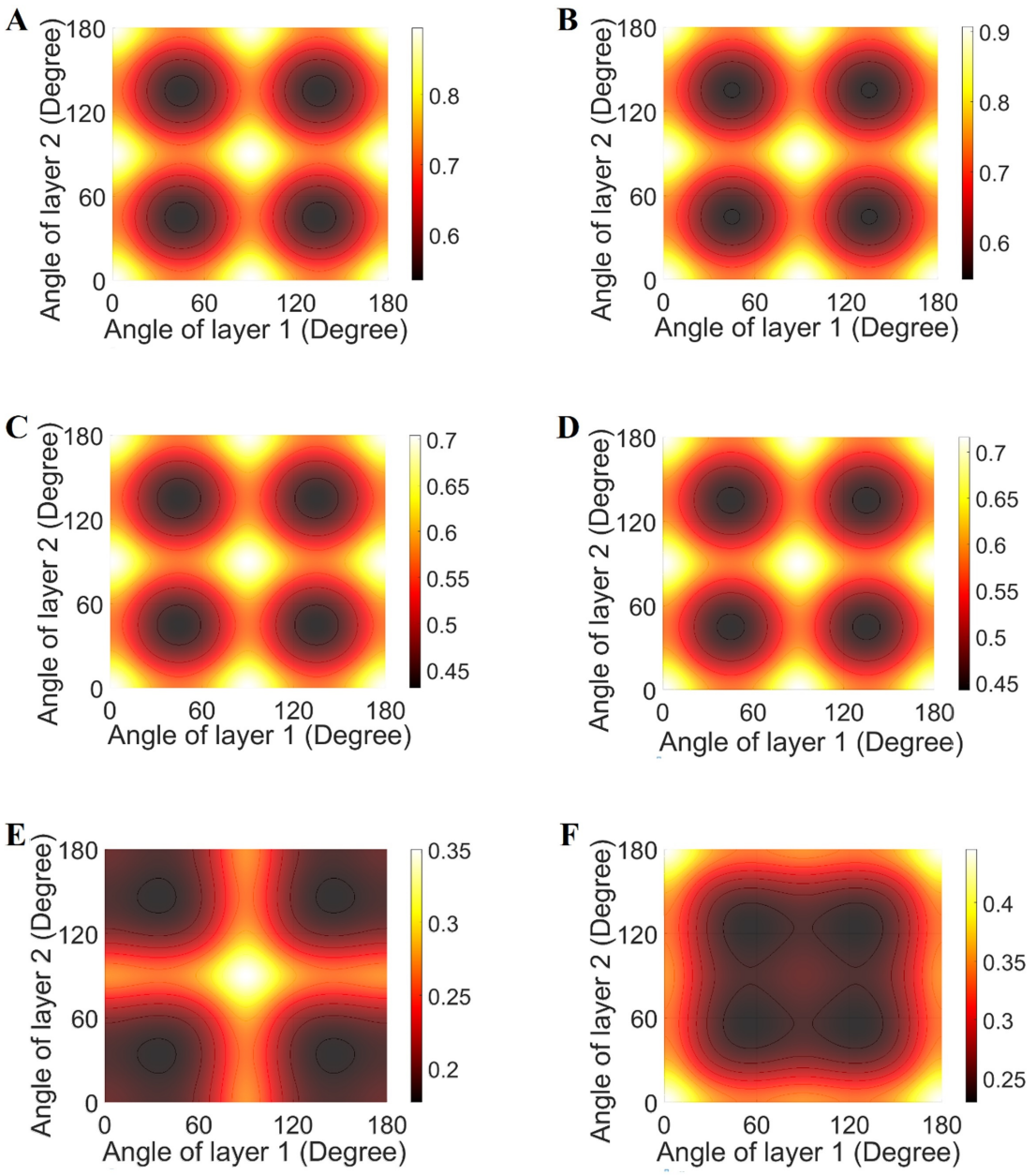

Figure S8: Young's modulus (TPa) of three-layer configurations, where stanene is at one of the layers without any rotation and the other two rotating layers are of same material other than stanene. (A) Young's modulus E_1 of three-layer stanene-graphene heterostructure (S/G/G) with a configuration of $[0°/\theta_2°/\theta_3°]$, where θ_2 and θ_3 represent the in-plane rotational angle of layer 2 and layer 3 respectively **(B)** Young's modulus E_2 of three-layer stanene-graphene heterostructure (S/G/G) with a configuration of $[0°/\theta_2°/\theta_3°]$, where θ_2 and θ_3 represent the in-plane rotational angle of layer 2 and layer 3 respectively **(C)** Young's modulus E_1 of three-layer stanene-hBN heterostructure (S/H/H) with a configuration of $[0°/\theta_2°/\theta_3°]$, where θ_2 and θ_3 represent the in-plane rotational angle of layer 2 and layer 3 respectively **(D)** Young's modulus E_2 of three-layer stanene-hBN heterostructure (S/H/H) with a configuration of $[0°/\theta_2°/\theta_3°]$, where θ_2 and θ_3 represent the in-plane rotational angle of layer 2 and layer 3 respectively **(E)** Young's modulus E_1 of three-layer stanene-MoS_2 heterostructure (S/M/M) with a configuration of $[0°/\theta_2°/\theta_3°]$, where θ_2 and θ_3 represent the in-plane rotational angle of layer 2 and layer 3 respectively **(F)** Young's modulus E_2 of three-layer stanene-MoS_2 heterostructure (S/M/M) with a configuration of $[0°/\theta_2°/\theta_3°]$, where θ_2 and θ_3 represent the in-plane rotational angle of layer 2 and layer 3 respectively.

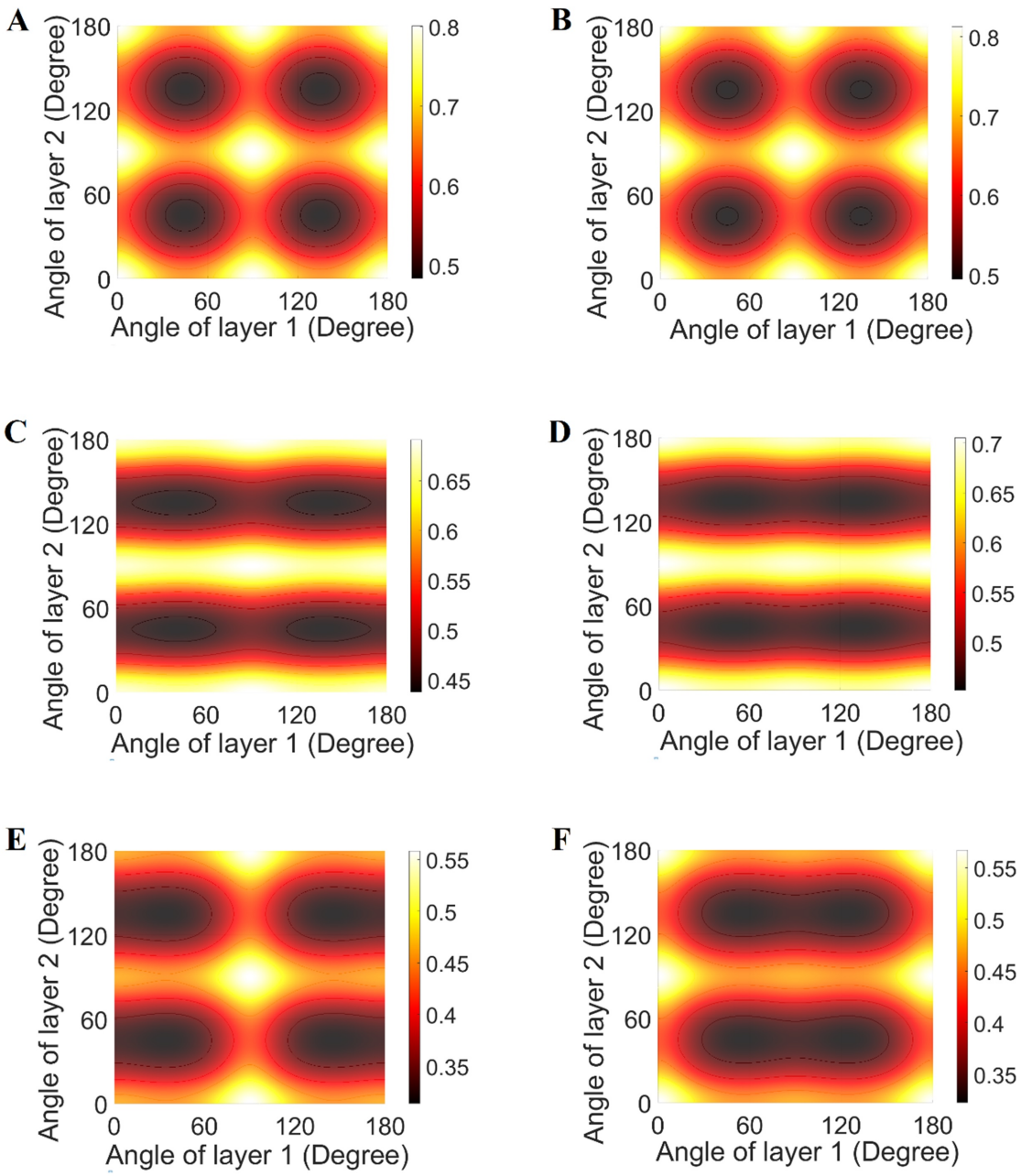

Figure S9: Young's modulus (TPa) of three-layer configurations, where stanene is at one of the layers without any rotation and one of the rotating layers is graphene. (A) Young's modulus E_1 of three-layer stanene-hBN-graphene heterostructure (S/G/H or S/H/G) with a configuration of $[0°/\theta_2°/\theta_3°]$, where θ_2 and θ_3 represent the in-plane rotational angle of layer 2 and layer 3 respectively **(B)** Young's modulus E_2 of three-layer stanene-hBN-graphene heterostructure (S/G/H or S/H/G) with a configuration of $[0°/\theta_2°/\theta_3°]$, where θ_2 and θ_3 represent the in-plane rotational angle of layer 2 and layer 3 respectively **(C)** Young's modulus E_1 of three-layer stanene-graphene heterostructure (S/G/S or S/S/G) with a configuration of $[0°/\theta_2°/\theta_3°]$, where θ_2 and θ_3 represent the in-plane rotational angle of layer 2 and layer 3 respectively **(D)** Young's modulus E_2 of three-layer stanene-graphene heterostructure (S/G/S or S/S/G) with a configuration of $[0°/\theta_2°/\theta_3°]$, where θ_2 and θ_3 represent the in-plane rotational angle of layer 2 and layer 3 respectively **(E)** Young's modulus E_1 of three-layer stanene-graphene-MoS_2 heterostructure (S/G/M or S/M/G) with a configuration of $[0°/\theta_2°/\theta_3°]$, where θ_2 and θ_3 represent the in-plane rotational angle of layer 2 and layer 3 respectively **(F)** Young's modulus E_2 of three-layer stanene-graphene-MoS_2 heterostructure (S/G/M or S/M/G) with a configuration of $[0°/\theta_2°/\theta_3°]$, where θ_2 and θ_3 represent the in-plane rotational angle of layer 2 and layer 3 respectively.

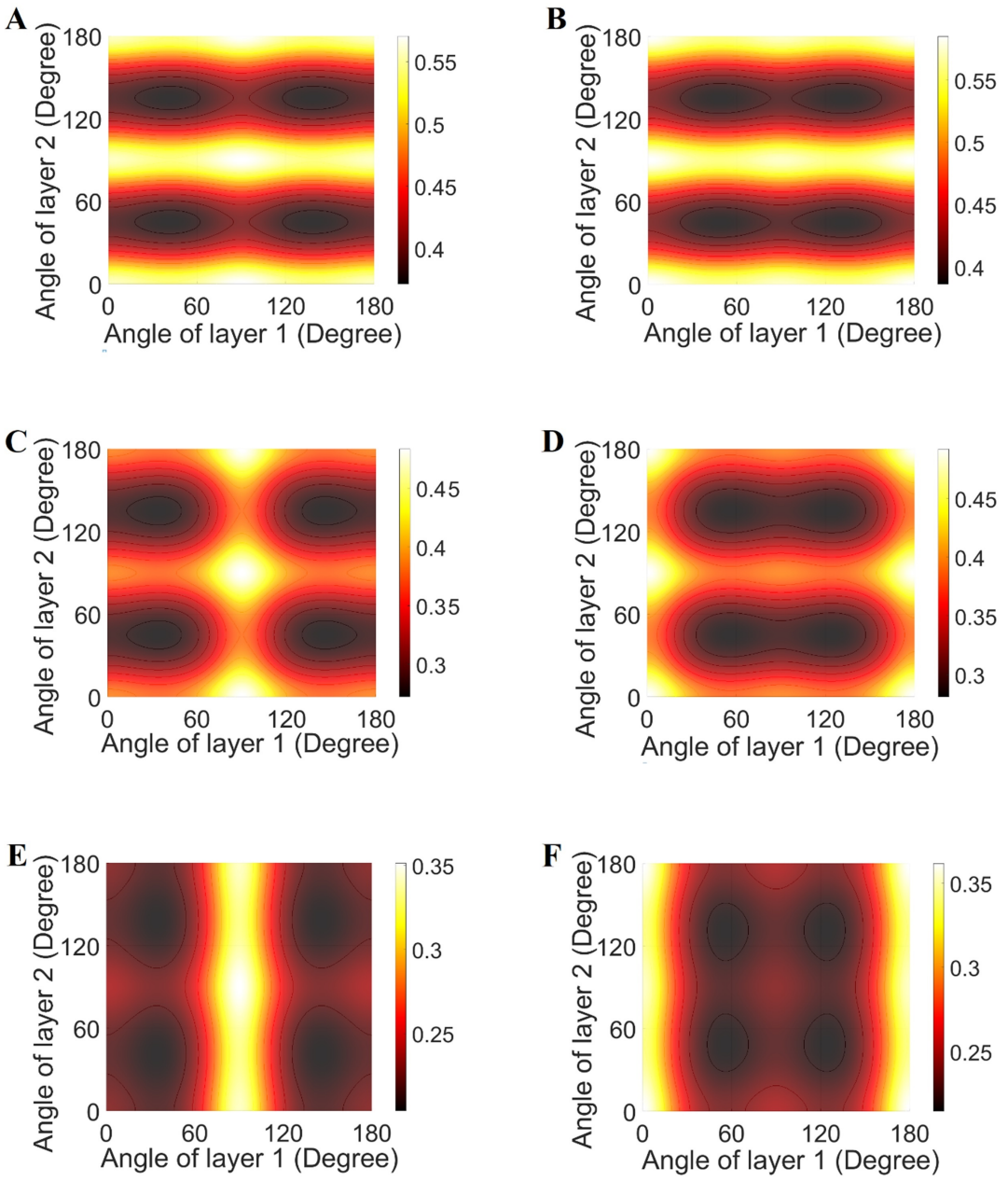

Figure S10: Young's modulus (TPa) of three-layer configurations, where stanene is at one of the layers without any rotation and the other two rotating layers are of two different materials other than graphene. (A) Young's modulus E_1 of three-layer stanene-hBN heterostructure (S/H/S or S/S/H) with a configuration of $[0°/\theta_2°/\theta_3°]$, where θ_2 and θ_3 represent the in-plane rotational angle of layer 2 and layer 3 respectively **(B)** Young's modulus E_2 of three-layer stanene-hBN heterostructure (S/H/S or S/S/H) with a configuration of $[0°/\theta_2°/\theta_3°]$, where θ_2 and θ_3 represent the in-plane rotational angle of layer 2 and layer 3 respectively **(C)** Young's modulus E_1 of three-layer stanene-hBN-MoS_2 heterostructure (S/H/M or S/M/H) with a configuration of $[0°/\theta_2°/\theta_3°]$, where θ_2 and θ_3 represent the in-plane rotational angle of layer 2 and layer 3 respectively **(D)** Young's modulus E_2 of three-layer stanene-hBN-MoS_2 heterostructure (S/H/M or S/M/H) with a configuration of $[0°/\theta_2°/\theta_3°]$, where θ_2 and θ_3 represent the in-plane rotational angle of layer 2 and layer 3 respectively **(E)** Young's modulus E_1 of three-layer stanene-MoS_2 heterostructure (S/S/M or S/M/S) with a configuration of $[0°/\theta_2°/\theta_3°]$, where θ_2 and θ_3 represent the in-plane rotational angle of layer 2 and layer 3 respectively **(F)** Young's modulus E_2 of three-layer stanene-MoS_2 heterostructure (S/S/M or S/M/S) with a configuration of $[0°/\theta_2°/\theta_3°]$, where θ_2 and θ_3 represent the in-plane rotational angle of layer 2 and layer 3 respectively.

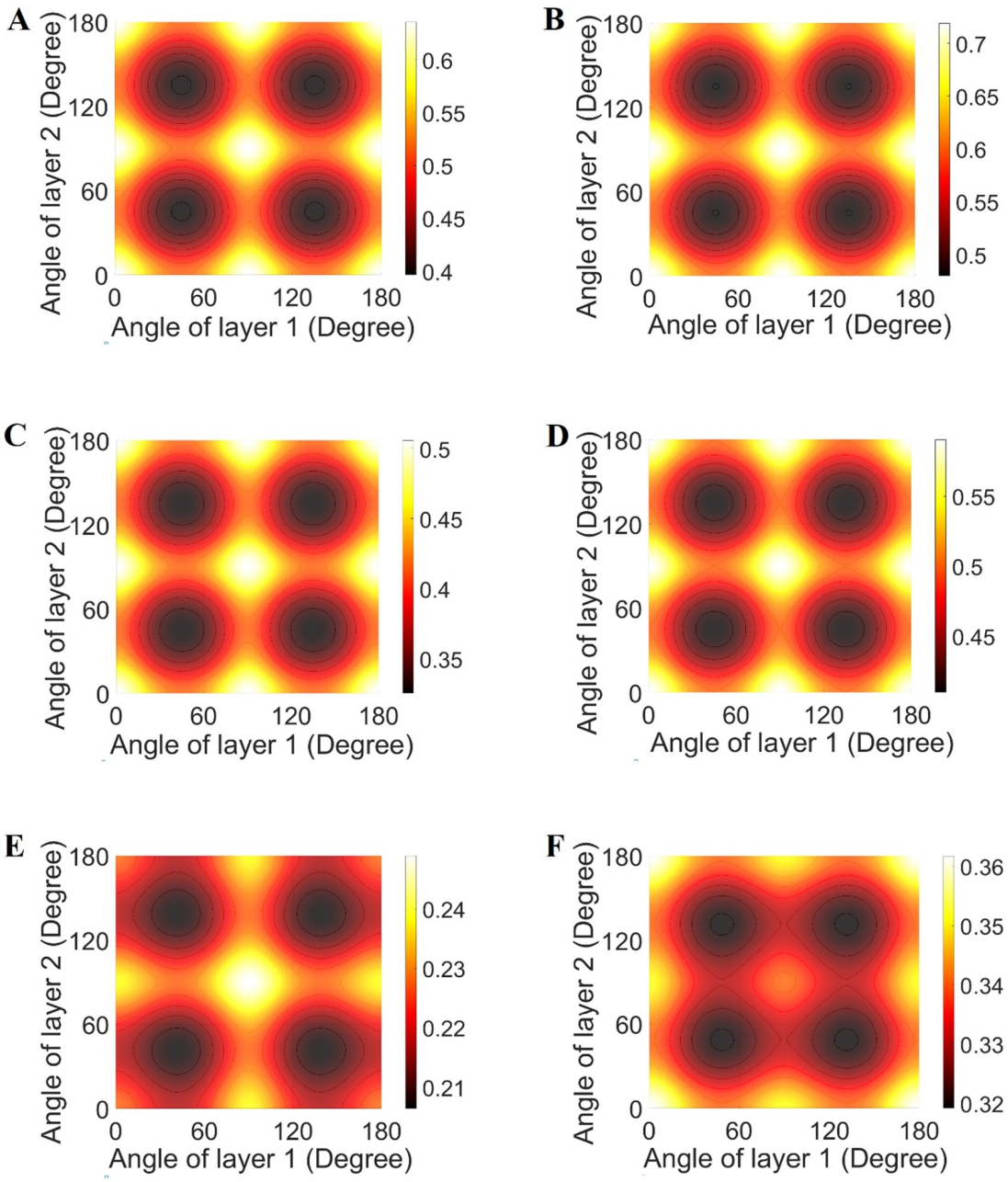

Figure S11: Young's modulus (TPa) of three-layer configurations, where MoS_2 is at one of the layers without any rotation and the other two rotating layers are of same material other than MoS_2. (A) Young's modulus E_1 of three-layer MoS_2-graphene heterostructure (M/G/G) with a configuration of $[0°/\theta_2°/\theta_3°]$, where θ_2 and θ_3 represent the in-plane rotational angle of layer 2 and layer 3 respectively **(B)** Young's modulus E_2 of three-layer MoS_2-graphene heterostructure (M/G/G) with a configuration of $[0°/\theta_2°/\theta_3°]$, where θ_2 and θ_3 represent the in-plane rotational angle of layer 2 and layer 3 respectively **(C)** Young's modulus E_1 of three-layer MoS_2-hBN heterostructure (M/H/H) with a configuration of $[0°/\theta_2°/\theta_3°]$, where θ_2 and θ_3 represent the in-plane rotational angle of layer 2 and layer 3 respectively **(D)** Young's modulus E_2 of three-layer MoS_2-hBN heterostructure (M/H/H) with a configuration of $[0°/\theta_2°/\theta_3°]$, where θ_2 and θ_3 represent the in-plane rotational angle of layer 2 and layer 3 respectively **(E)** Young's modulus E_1 of three-layer MoS_2-stanene heterostructure (M/S/S) with a configuration of $[0°/\theta_2°/\theta_3°]$, where θ_2 and θ_3 represent the in-plane rotational angle of layer 2 and layer 3 respectively **(F)** Young's modulus E_2 of three-layer MoS_2-stanene heterostructure (M/S/S) with a configuration of $[0°/\theta_2°/\theta_3°]$, where θ_2 and θ_3 represent the in-plane rotational angle of layer 2 and layer 3 respectively.

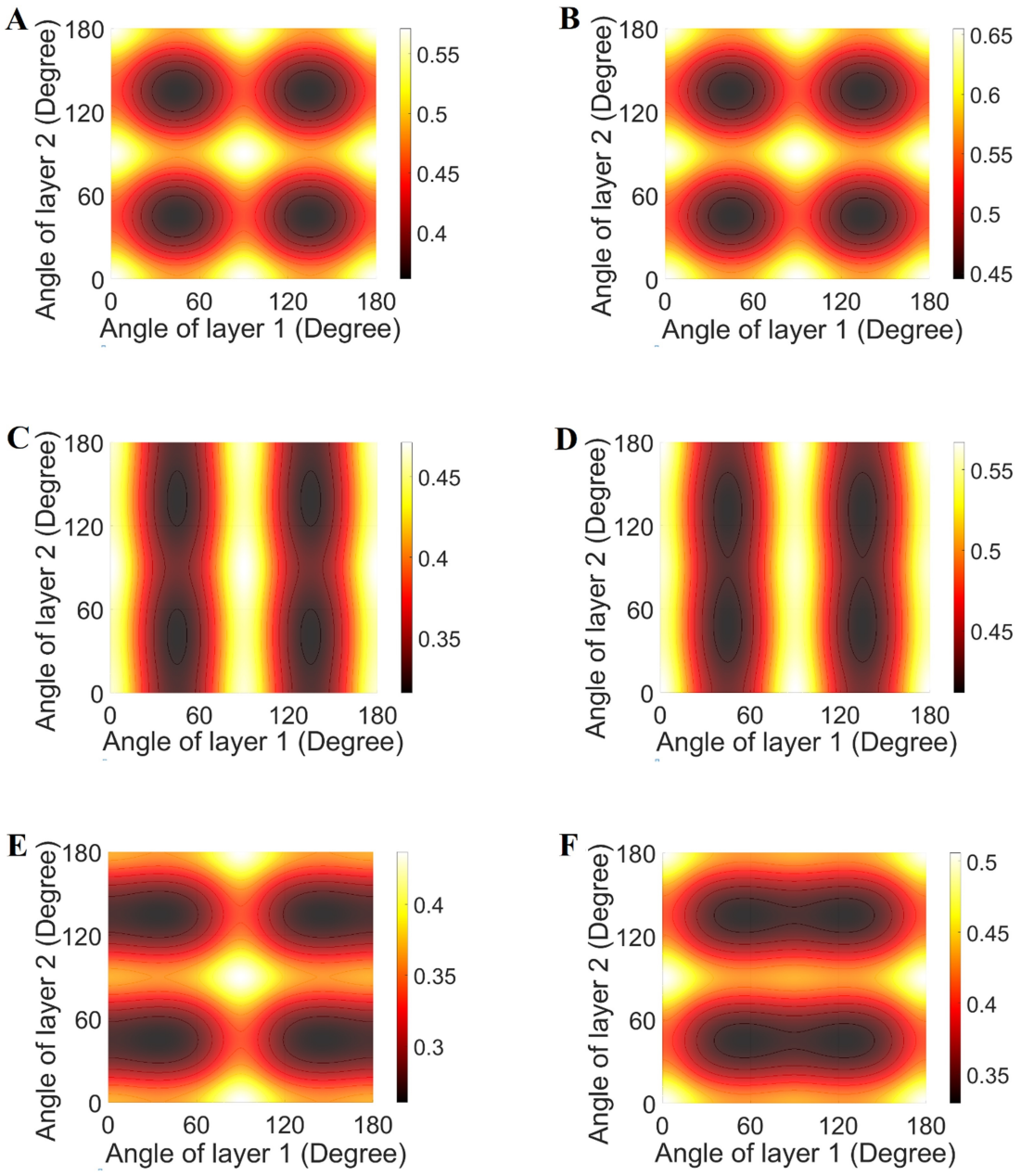

Figure S12: Young's modulus (TPa) of three-layer configurations, where MoS_2 is at one of the layers without any rotation and one of the rotating layers is graphene. (A) Young's modulus E_1 of three-layer MoS_2-hBN-graphene heterostructure (M/G/H or M/H/G) with a configuration of $[0°/\theta_2°/\theta_3°]$, where θ_2 and θ_3 represent the in-plane rotational angle of layer 2 and layer 3 respectively **(B)** Young's modulus E_2 of three-layer MoS_2-hBN-graphene heterostructure (M/G/H or M/H/G) with a configuration of $[0°/\theta_2°/\theta_3°]$, where θ_2 and θ_3 represent the in-plane rotational angle of layer 2 and layer 3 respectively **(C)** Young's modulus E_1 of three-layer MoS_2-stanene-graphene heterostructure (M/G/S or M/S/G) with a configuration of $[0°/\theta_2°/\theta_3°]$, where θ_2 and θ_3 represent the in-plane rotational angle of layer 2 and layer 3 respectively **(D)** Young's modulus E_2 of three-layer MoS_2-stanene-graphene heterostructure (M/G/S or M/S/G) with a configuration of $[0°/\theta_2°/\theta_3°]$, where θ_2 and θ_3 represent the in-plane rotational angle of layer 2 and layer 3 respectively **(E)** Young's modulus E_1 of three-layer graphene-MoS_2 heterostructure (M/G/M or M/M/G) with a configuration of $[0°/\theta_2°/\theta_3°]$, where θ_2 and θ_3 represent the in-plane rotational angle of layer 2 and layer 3 respectively **(F)** Young's modulus E_2 of three-layer graphene-MoS_2 heterostructure (M/G/M or M/M/G) with a configuration of $[0°/\theta_2°/\theta_3°]$, where θ_2 and θ_3 represent the in-plane rotational angle of layer 2 and layer 3 respectively.

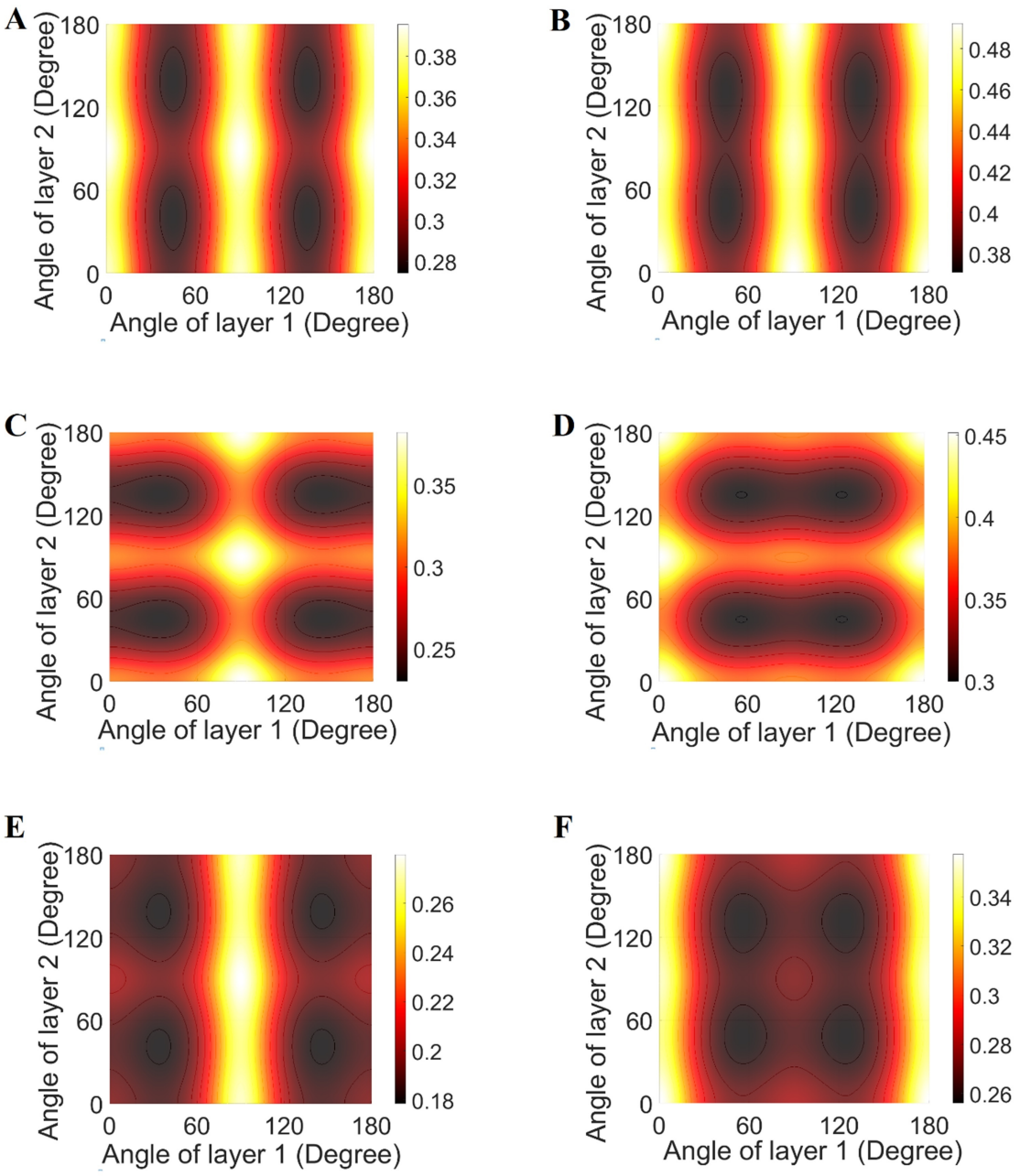

Figure S13: Young's modulus (TPa) of three-layer configurations, where MoS_2 is at one of the layers without any rotation and the other two rotating layers are of two different materials other than graphene. **(A)** Young's modulus E_1 of three-layer MoS_2-stanene-hBN heterostructure (M/H/S or M/S/H) with a configuration of $[0°/\theta_2°/\theta_3°]$, where θ_2 and θ_3 represent the in-plane rotational angle of layer 2 and layer 3 respectively **(B)** Young's modulus E_2 of three-layer MoS_2-stanene-hBN heterostructure (M/H/S or M/S/H) with a configuration of $[0°/\theta_2°/\theta_3°]$, where θ_2 and θ_3 represent the in-plane rotational angle of layer 2 and layer 3 respectively **(C)** Young's modulus E_1 of three-layer hBN-MoS_2 heterostructure (M/H/M or M/M/H) with a configuration of $[0°/\theta_2°/\theta_3°]$, where θ_2 and θ_3 represent the in-plane rotational angle of layer 2 and layer 3 respectively **(D)** Young's modulus E_2 of three-layer hBN-MoS_2 heterostructure (M/H/M or M/M/H) with a configuration of $[0°/\theta_2°/\theta_3°]$, where θ_2 and θ_3 represent the in-plane rotational angle of layer 2 and layer 3 respectively **(E)** Young's modulus E_1 of three-layer stanene-MoS_2 heterostructure (M/S/M or M/M/S) with a configuration of $[0°/\theta_2°/\theta_3°]$, where θ_2 and θ_3 represent the in-plane rotational angle of layer 2 and layer 3 respectively **(F)** Young's modulus E_2 of three-layer stanene-MoS_2 heterostructure (M/S/M or M/M/S) with a configuration of $[0°/\theta_2°/\theta_3°]$, where θ_2 and θ_3 represent the in-plane rotational angle of layer 2 and layer 3 respectively.

one layer of multiplanar 2D material is expected to show different E_1 and E_2 values (corresponding to $\theta = 0^\circ$ or any particular θ value). The Young's moduli E_1 and E_2 become equal when all the layers are composed of only monoplanar configurations, though different monoplanar 2D material could be present in such a heterostructure.

Acknowledgements

TM and SN acknowledge the Initiation grants received from IIT Kanpur and IIT Bombay, respectively. SA acknowledges the support of UK-India Education and Research Initiative through grant number UKIERI/P1212.

Competing interests

The authors declare no competing financial interests.

References

[1] Chang, T. & Gao, H. Size-dependent elastic properties of a single-walled carbon nanotube via a molecular mechanics model. *Journal of the Mechanics and Physics of Solids* **51**, 1059–1074 (2003).

[2] Shokrieh, M. M. & Rafiee, R. Prediction of young's modulus of graphene sheets and carbon nanotubes using nanoscale continuum mechanics approach. *Materials & Design* **31**, 790–795 (2010).

[3] Mukhopadhyay, T., Mahata, A., Adhikari, S. & Zaeem, M. A. Effective elastic properties of two dimensional multiplanar hexagonal nanostructures. *2D Materials* **4**, 025006 (2017).

[4] Gelin, B. R. *Molecular Modeling of Polymer Structures and Properties* (Hanser Gardner Publications, 1994).

[5] Mukhopadhyay, T. and Mahata A. and Asle Zaeem M. and Adhikari, S. Effective mechanical properties of multilayer nano-heterostructures. *Scientific Reports*, 7:15818, 2017.